iScience

CellPress
OPEN ACCESS

Article

The 3D Reconstruction of *Pocillopora* Colony Sheds Light on the Growth Pattern of This Reef-Building Coral

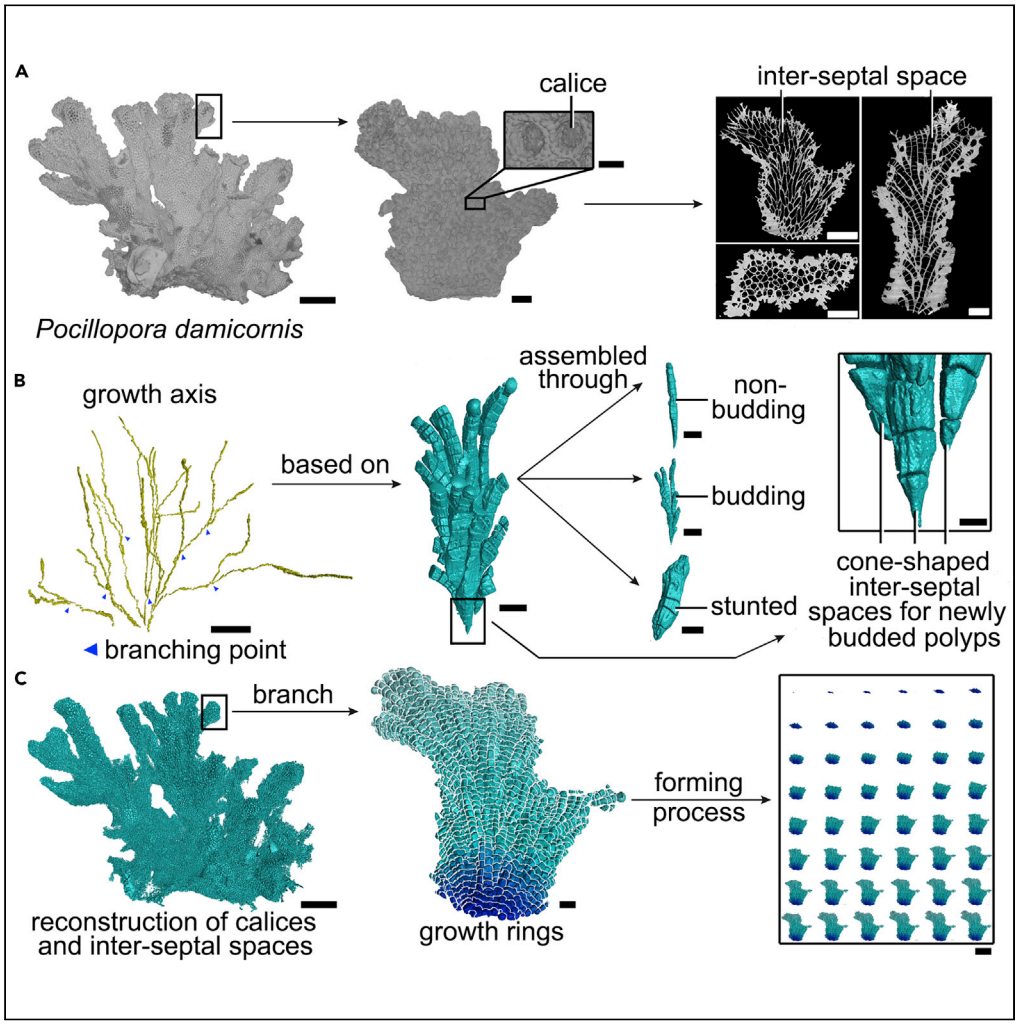

Yixin Li, Tingyu Han, Kun Bi, ..., Jing Lu, Chunpeng He, Zuhong Lu

lujing@ivpp.ac.cn (J.L.)
cphe@seu.edu.cn (C.H.)
zhlu@seu.edu.cn (Z.L.)

HIGHLIGHTS

We use high-resolution computed tomography to investigate coral forming and polyp budding processes

The calice reconstruction shows coral growth patterns and budding information

Our work visualizes the growth pattern of *Pocillopora damicornis*

High-resolution computed tomography is a method for future reef-building coral studies

Li et al., iScience *23*, 101069
June 26, 2020
https://doi.org/10.1016/j.isci.2020.101069

iScience

CellPress
OPEN ACCESS

Article

The 3D Reconstruction of *Pocillopora* Colony Sheds Light on the Growth Pattern of This Reef-Building Coral

Yixin Li,[1] Tingyu Han,[1] Kun Bi,[1] Kun Liang,[2] Junyuan Chen,[2] Jing Lu,[3,4,*] Chunpeng He,[1,*] and Zuhong Lu[1,5,*]

SUMMARY

Coral reefs are formed by living polyps, and understanding the dynamic processes behind the reefs is crucial for marine ecosystem restoration. However, these processes are still unclear because the growth and budding patterns of living polyps are poorly known. Here, we investigate the growth pattern of a widely distributed reef-building coral *Pocillopora damicornis* from Xisha Islands using high-resolution computed tomography. We examine the corallites in a single corallum of the species in detail, to interpret the budding, growth, and distribution pattern of the polyps, to reconstruct the growth pattern of this important reef-building species. Our results reveal a three-stage growth pattern of *P. damicornis*, based on different growth bundles that are secreted by polyps along the dichotomous growth axes of the corallites. Our work on the three-dimensional reconstruction of calice and inter-septal space structure of *P. damicornis* sheds lights on its reef-building processes by reconstructing the budding patterns.

INTRODUCTION

Reef-building scleractinian corals provide complex three-dimensional niches for various species (Costanza et al., 2014; Ellison et al., 2005; Knowlton et al., 2010; Weis et al., 2008; Graham, 2014). However, coral reefs are currently declining globally because of the climate change (Carpenter et al., 2008; Kleypas et al., 1999; Maynard et al., 2015), especially owing to the intensification of El Niño (Jokiel and Coles, 1977; Bellwood et al., 2004; De'ath et al., 2012), water-quality deterioration (Tambutté et al., 2015; Mollica, 2018), and overexploitation (Natt et al., 2017; Robinson et al., 2017). Studies on the biochemical processes governing coral reef and their ecological health under environmental changes are therefore undoubtedly in the spotlight (Fabricius et al., 2010).

The reef-building scleractinian coral *Pocillopora damicornis* is widespread in the Indo-Pacific ocean and is one of the most abundant and widely distributed species in the world (Veron and Staffordsmith, 2000). This coral has a high growth rate, which is advantageous in the competition to survive (Cunning et al., 2018). *P. damicornis* has stronger defenses against bleaching and is better adapted to environmental changes than most other coral species (Carpenter et al., 2008). In some regions of Xisha Islands where external disturbances such as the El Niño and ocean pollution have overwhelmed the capacity of corals to recover from damage, some stress-tolerant corals like *P. damicornis* show better environmental adaptability and become the dominant coral species instead of the most common species like *Montipora* and *Acropora* belonging to the family *Acroporidae* (Kayal et al., 2015; Bramanti and Edmunds, 2016; Adjeroud et al., 2018). This makes *P. damicornis* an important animal, and various aspects concerning this species should be studied, such as their speciation (Johnston et al., 2017; Schmidt-Roach et al., 2014), reproduction (Miller and Ayre, 2004; Schmidt-Roach et al., 2012; Combosch and Vollmer, 2013), symbiosis (Cunning and Baker, 2012; Kopp, 2015; Brener-Raffalli et al., 2018), and population genetics (Stoddart, 1984; Souter et al., 2009; Thomas et al., 2017). Recently, researchers have performed comprehensive studies on *P. damicornis* including their genomics (Torda et al., 2013; Combosch and Vollmer, 2015; Wilkinson et al., 2015; Mass et al., 2016; Crowder et al., 2017; Yuan et al., 2017; Zhang et al., 2018), polyp metabolism (Lecointe et al., 2013; Kvitt et al., 2015), zooxanthellae (Zhou et al., 2017), disease resistance (Ben-Haim et al., 2003), adaptation to environmental change (Crowder et al., 2014; Rivest and Hofmann, 2014; Paz-García et al., 2015; Rodríguez-Villalobos et al., 2016;

[1]State Key Laboratory of Bioelectronics, School of Biological Science and Medical Engineering, Southeast University, Nanjing 210096, China

[2]Nanjing Institute of Paleontology and Geology, 39 East Beijing Road, Nanjing 210008, China

[3]Key Laboratory of Vertebrate Evolution and Human Origins of Chinese Academy of Sciences, Institute of Vertebrate Paleontology and Paleoanthropology, Chinese Academy of Sciences, PO Box 643, Beijing 100044, China

[4]CAS Center for Excellence in Life and Paleoenvironment, Beijing 100044, China

[5]Lead Contact

*Correspondence: lujing@ivpp.ac.cn (J.L.), cphe@seu.edu.cn (C.H.), zhlu@seu.edu.cn (Z.L.)

https://doi.org/10.1016/j.isci.2020.101069

Traylor-Knowles, 2016; Zhou et al., 2016, 2018; Yu et al., 2017), and integration with microfluidic systems (Helman et al., 2008; Mass et al., 2012; Shapiro et al., 2016) and electronic sensors (Szabó et al., 2014; Mu et al., 2017).

However, although *P. damicornis* is one of the most extensively studied coral species in terms of overall macromorphological and microarchitectural details (Schmidt-Roach et al., 2013; Veron and Pichon, 1976), the structures of calice and inter-septal space and the relationship between coral growth pattern and its skeleton are still poorly known owing to the limitations of the technology. Most studies on coral structures are based on small samples at low resolutions. These studies are limited by the equipment such as optical microscopes (Welsh et al., 2017), scanning electron microscopes (SEMs) (Bonesso et al., 2017), and industrial computed tomography with low resolution (Chindapol et al., 2013), which did not provide a precise and comprehensive overview on the coral structures owing to limited resolution and scales. To study the growth patterns of the corals, traditional micro-CT has been used in several studies (Beuck et al., 2007; Knackstedt et al., 2006; Kruszynski et al., 2006, 2007; Nishikawa et al., 2009). However, as micro-CT technology was still developing when these studies were performed, the reconstructed images revealed only the exterior of the coralla instead of detailed internal calice structures and growth patterns.

Recently, with the development of modern technology, high-resolution computed tomography (HRCT) has gained increasing attention in biological research for its high-resolution and nondestructive nature. Previous works based on HRCT on the internal skeletal structures of certain corals increase our knowledge on the coral skeletons (Janiszewska et al., 2011, 2013; Tambutté et al., 2015). However, owing to lack of virtual segmentation and further investigation, our understanding of the 3D skeletal structures of the corals remains poor. Here, we investigate the three-dimensional skeletal structures of reef-building coral *P. damicornis* from Xisha Island, China, and reconstruct its calice and internal inter-septal space network by using HRCT and virtual segmentation, which helps us to understand the budding, growth, and distribution information of the polyps during the growth process (Figure S1).

RESULTS

General Morphological Structure of *P. damicornis*

We assembled a 3D morphological structure incorporating details at both macroscopic and microscopic scales by reconstructing a single *P. damicornis* corallum with a size of approximately 3,600 cm^3 (Figure 1A). The reconstructed image presents the complete form of the original coral skeleton details of surface bulges and calices, which significantly facilitates the study of its skeleton and biological characteristics. There are multiple calices closely packed on the surface, and a single polyp grows in each calice. The connections between the calices are realized by desmocytes that fasten the coral soft tissue to the skeleton. Coralla of *P. damicornis* have many branches, and the gaps between these branches are often the habitat of small aquatic organisms such as shrimps and crabs (Figure 1A).

To study the internal calices more clearly, we scan two small branches from a large corallum of *P. damicornis* and reconstruct their 3D structures at a high resolution (Figures 1B and 1C) to further study the calices and internal inter-septal spaces from the microscopic perspective.

Skeletal and Calice and Internal Inter-Septal Space Structures of *P. damicornis*

To observe the skeleton and internal calices, we obtained 3D, cross-sectional, and slice images at multiple branches of the reconstructed *P. damicornis* models (Figures 1C–1F and S2A). There are no holes among the coral coenosteums, and each polyp has its own distinguishable calice, which is completely sealed off. Thus, there is no direct connection between adjacent calices. All these calices and inter-septal spaces record the spatiotemporal growth of each individual polyp in this colony. Owing to separation of tabulae, the living polyps are present only at the surface of the colony, and the interior spaces do not contain living polyps. Additionally, the corallites are much thicker than the coenosteums among all these skeleton structures (Figures 1D–1F).

By measuring the diameter on the top of the calice, we calculated the corallite diameter (Figure 1C). We also obtain the aboral surface diameter and speculate the height of polyps using these measurements (Figures S3A–S3C), therefore, to determine the calicular volume between last tabula and the calicular margin, which cannot be determined by polyp bailout or SEM techniques (Figures S3D–S3F). According to the

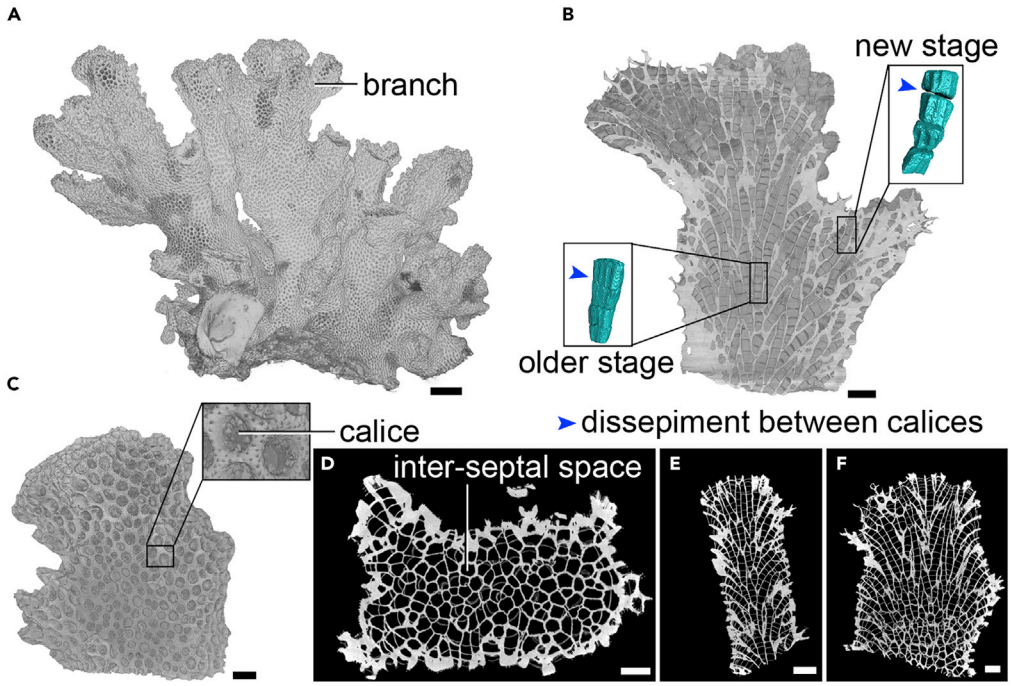

Figure 1. High-Resolution Micro-CT Reconstruction of *P. damicornis*

(A) Reconstruction skeleton image of the entire *P. damicornis* sample.

(B) Front vertical sectional image of branchlet one, with two calice and inter-septal space reconstructions. We reconstructed and compared two structures, including a newly built one at the edge and an older one deep inside the colony. There are apparent separations between the newly formed calices and inter-septal spaces, whereas the separations are not distinct between older inter-septal spaces.

(C) 3D reconstruction of branchlet two and the calice of its surface polyp. By measuring the diameter at the opening of the hole, it is possible to directly obtain visual measurement data such as the diameter of polyp oral surface in a natural, undistorted state. Diameter of polyp abactinal surface and vertical height can be seen in Figure S3. This study effectively determines the volume of polyp calice and body size, which cannot be determined by polyp bailout or SEM (see Figure S3 for full image).

(D) Top view image of the *P. damicornis* branchlet reconstruction model.

(E) Lateral sectional image of the *P. damicornis* branchlet reconstruction model.

(F) Front sectional image of the *P. damicornis* branchlet reconstruction model.

Scale bars: (A) 1 cm; (B) 2 mm; (C) 2 mm; (D–F) 2 mm.

reconstructed model, the diameters of both the oral and aboral surfaces are generally between 0.5 and 1 mm, and the polyp heights are between 0.1 and 0.6 mm.

In the reconstructed 3D images, bamboo-like calice and inter-septal space structures on the same branch of *P. damicornis* branch out in a generally alternate way (Figure S2A). We selected one part of the coral skeleton to reconstruct a 3D model. To show the internal structure of the coral, we dissected the selected coral skeleton along its vertical axis, revealing the internal bamboo-like structures; for more detailed observations, we also investigated a vertical section (Figure S2B).

Growth Patterns and Internal Network of *P. damicornis*

To investigate the growth pattern of polyps, we reconstructed the calices and inter-septal spaces chamber by chamber (Figures 2, S4, and S5). The reconstructed results suggest that the coral skeleton can be divided into two types according to the stage of mineralization (Figure 1B): the first one is new, containing the newly built calices and inter-septal spaces at the surface layer, whereas the other is older, containing the older inter-septal spaces inside the colony. The newly formed calices and inter-septal spaces are at the surface of the coral and they are closely spaced, with small gaps indicating the existence of dissepiments (Wells, 1969). The basic morphological structure of the inner (older) inter-septal space is like those of the new ones, but their dissepiments are thinner. This phenomenon shows that, along with the colony growth via

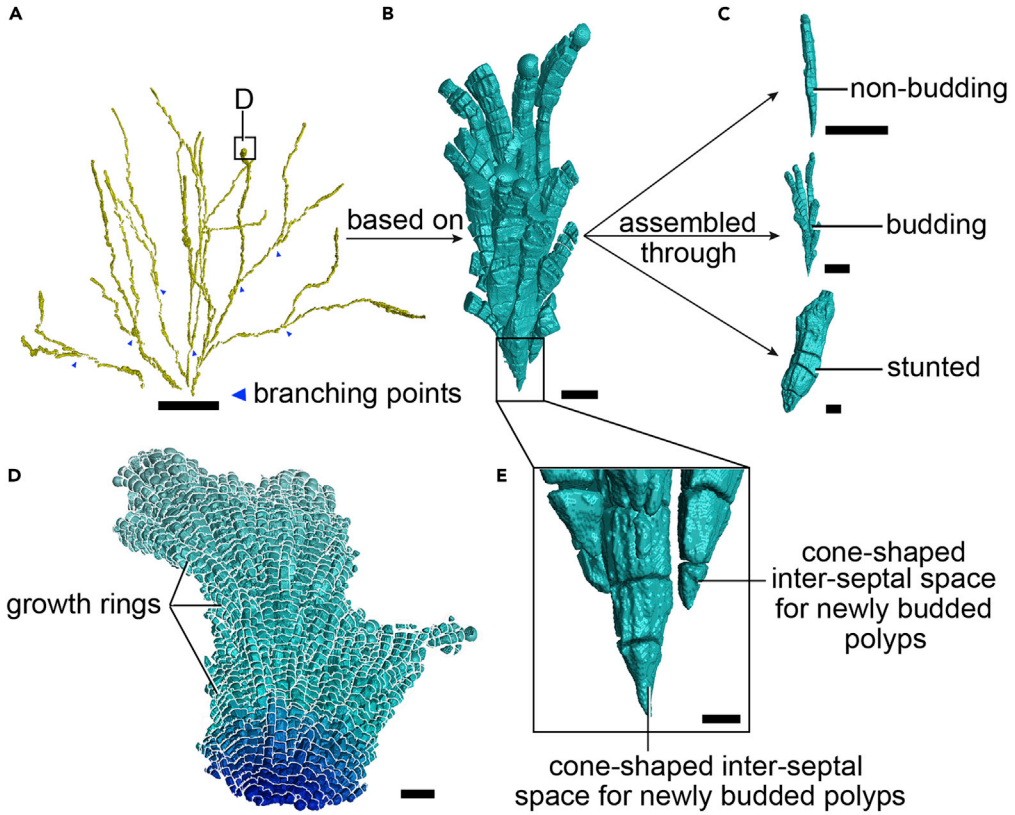

Figure 2. Growth Pattern of *P. damicornis*

(A) The entire calice and inter-septal space that grows from a growing point to the surface of the coral of the *P. damicornis* branchlet showing the three-stage growth pattern of *P. damicornis* polyps. At this scale, the branching of *P. damicornis* is dichotomous, growing generally in two directions with many smaller branches budding from minor growth axes. The blue arrows mark the branching points of the growth axes.

(B and C) (B) The growth bundle, which is the core structure of coral growth, based on growth bundles along the dichotomous growth axes, assembled through multiple growth types (C).

(D) Growth rings of *P. damicornis*.

(E) Amplifying lower edge of the *P. damicornis* growth bundle, showing the newly divided calices growing into larger column-shaped structures as polyp growth volume increases, the key feature for distinguishing the budding branch and spatial distribution of coral polyps, and is the basis for constructing the *P. damicornis* calice and inter-septal space network in virtual 3D reconstructions.

Scale bars: (A) 1 cm; (B) 1 mm; (C) 500 μm; (D) 2 mm; (E) 200 μm.

asexual reproduction, the dissepiments between adjacent inter-septal spaces become thinner, indicating the process of coral skeletal formation.

During the process of reconstruction of *P. damicornis*, we notice an important feature of the species that shows that the living polyps extend to the surface of the coral from their initial growth points (budding sites), whereas no polyp dies in the internal part of the coral. This indicates that coral growth is holistic at the macro level, although individual polyps are shown to be physically isolated from each other at the micro level. In addition, we identified several distinct growth types of *P. damicornis* according to the shape of calices and inter-septal spaces, including budding, nonbudding, and stunted growth types (Figure 2A). The budding and nonbudding types contain more inter-septal spaces than the stunted type. The budding type can undergo asexual reproduction, whereas the nonbudding type cannot. The inter-septal spaces of stunted growth type are much shorter than those two growth-type calices and are distributed near the surface of the colony. There are only a few calice and inter-septal space in the stunted type during the growth of the polyps.

To further investigate the growth pattern of coral polyps, we reconstructed the interior calices and inter-septal spaces of a smaller specimen in precise detail (Figure 2). We reconstructed a complete inter-septal

space from its original growth point to the surface calice of the colony in a coral branchlet. We name a group of polyps with synchronized growth as "growth bundle" (Figure 2A). The growth bundle shown in Figure 2 contains all of the growth types described above. The budding growth-type polyps are most commonly found in the interior of the bundle, which is the point of origin of coral growth. The nonbudding growth-type polyps are at the periphery of the bundle. The newly budded polyps have relatively small, inverted cone-shaped inter-septal spaces, and they grow gradually into larger ones (Figure 2C). The inverted cone-shaped inter-septal spaces are important to discern the budding of polyps and are fundamental for the 3D reconstruction relationship of polyps in *P. damicornis* at a large scale, including the budding, growth, and distribution of polyps that form an entire interactional network, which we called internal calice and inter-septal space network. This characteristic makes it possible to capture the behaviors of all the polyps in one corallum of *P. damicornis* by reconstruction, and budding sites can be accurately recorded regardless of the fate of certain individual polyp.

The vertical growth of *P. damicornis* shows a clear direction. We noticed that each *P. damicornis* polyp grows along an axis. The direction of the axis points to the direction of the growth of the branch. Each polyp grows along the growth axis rather than toward the light directly. Polyps growing in the direction of the growth axis will continuously build new calices, whereas those polyps deviating from the growth axis commonly stop after four or five inter-septal spaces to mineralize the corallite; therefore, the side branches of *P. damicornis* become thickened. When the colony of *P. damicornis* branches, its growth axis is also divided, suggesting that the polyps in each of the new branches grow into different directions. We selected each polyp calice at the top of the branch and traced the growth process of each polyp. In the reconstruction model, we build the large-scale internal growth axis structure of *P. damicornis* and present the growth direction of each branch (Figure 2A). It is found that not all growth axes are sunlight-oriented. The polyps grow toward the direction that maximizes the light-receiving area of the entire colony to improve the sunlight utilization and survive under strong competitions.

We notice that all the coral branches split into two during corallite increase. There are no tripartite or any other kind of increase during the growth of the colony. Although many buds branch out along smaller growth axes, only two major growth directions remain under large-scale conditions (Figure 2A). Different environmental conditions will affect the internal calices and inter-septal spaces of branches on the same coral. Branchlet reconstruction models can be divided into four sections: (1) low light mineralization area, (2) low light growth area, (3) light growth area, and (4) light mineralization area (Figure 3 and Data S1). A comparison of measurement data from different sections shows that growth areas 2 and 3 have higher average values than those from the mineralization areas 1 and 4, indicating that mineralization accumulates and fills the inter-septal spaces of the coral skeleton. Light areas 3 and 4 have higher average volume, diameter, and surface area than those of the low light areas 1 and 2, indicating that polyps exposed to light build larger calices than those not exposed to light and show better growth activity.

A significant feature of the polyp behavior is synchrony in growth, in which all polyps spend a similar amount of time producing a chamber. The stratified structure of the skeleton is a direct result of this synchronous growth. To investigate this characteristic, we divided a branchlet into 48 layers and simulated the outline of coral polyps in each layer (Figure S4 and Video S1). We obtained coral growth rings by simulating the growth process from each of the 48 layers (Figure S4). We perform a statistical analysis of the diameter and volume of calices and inter-septal spaces between dissepiments in the 48-layer *P. damicornis* colony (Data S1), then we calculate the average diameters and volumes of the calices and inter-septal spaces in each layer and illustrate using line chats on these data (Figure S6; Table S1). Through this way, the growth ring-forming process of a reef-building coral has been visualized and is of great significance for the yearly, seasonal, and monthly growth studies of reef-building corals.

DISCUSSION

Growth Patterns of *P. damicornis*

The microscale structures of a corallum of *P. damicornis* is revealed by HRCT, which enables us to reconstruct a high-precision 3D model for this species (Figure 1). The rendered internal calices and inter-septal spaces of *P. damicornis* (Figures 1, 2, and S4) provide several insights on the formation of coral reefs. Our analysis of the skeleton and calice of *P. damicornis* shows that the corallite is sealed and calices are disconnected from each other. This finding demonstrates that the polyps grow independent from each other at the micro level.

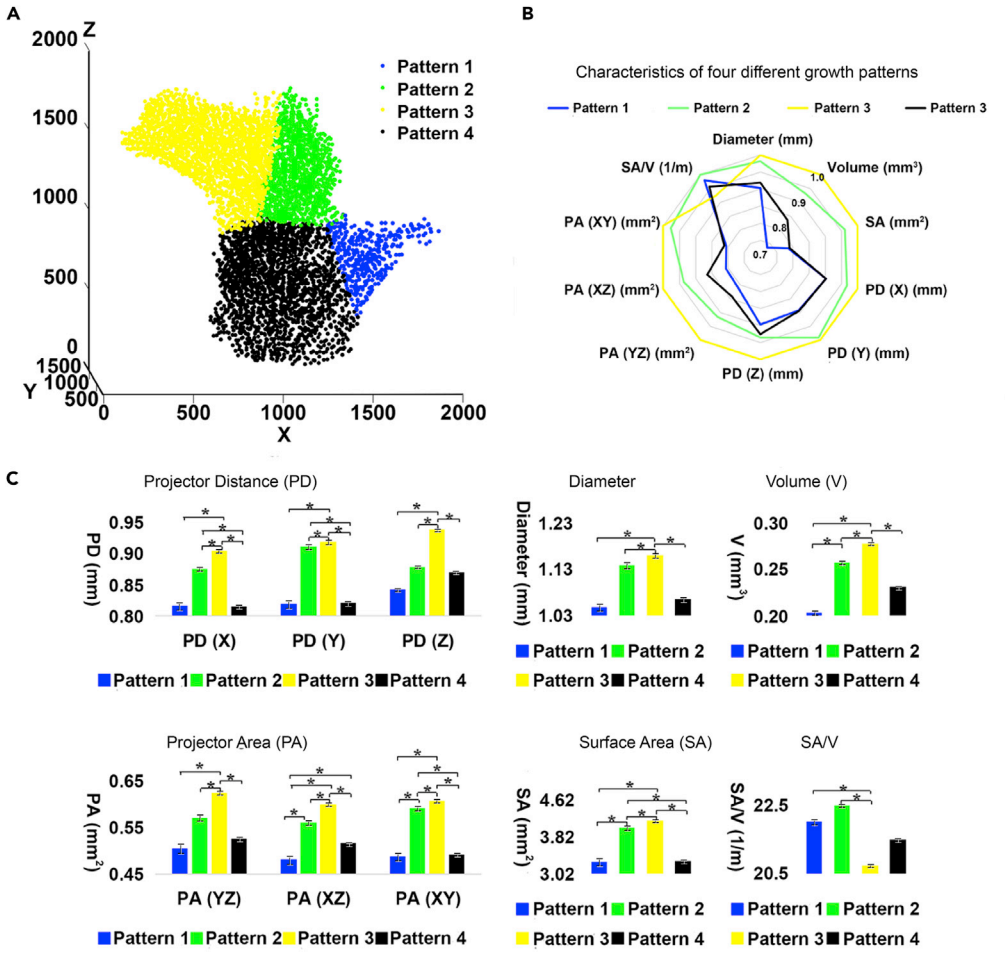

Figure 3. Cluster Analysis of *P. damicornis* Calice and Inter-Septal Space Obtained by Iterative Self-Organizing Data Analysis (ISODATA)

(A) We analyze the reconstruction calices and inter-septal spaces of coral branchlets (shown in Figure 1B) from the perspectives of their diameter; volume; surface area; surface-volume ratio; spatial coordinates of the X, Y, and Z axes; projection distances along the X, Y, and Z axes; and projected areas on the XY, XZ, and YZ planes. The branchlet reconstruction models are divided into four sections: (1) low light mineralization area, (2) low light growth area, (3) light growth area, (4) light mineralization area.

(B) Radar chart of the four sections. Growth areas 2 and 3 have higher average measurements than mineralization areas 1 and 4, indicating that mineralization accumulates and fills the inter-septal spaces of the coral skeleton. Light areas 3 and 4 have higher average measurements than low light areas 1 and 2, indicating that polyps exposed to light grow better and that light is significant for coral growth.

(C) Ten histograms reflecting the data comparisons of four sections. We calculate the average of the data from 5,648 reconstruction calice and inter-septal spaces as the mean, whereas the error bars are standard deviation. The type of statistical test is independent-samples t test. "*" marks in the figure means $p < 0.05$ between the two data groups.

However, although corallites are not related to each other at the micro level, they are uniformly regulated during growth because all living polyps extend to the surface of the coral from their initial growth point with no polyp death present in the internal part of the coral. The growth pattern of *Pocillopora* can be recognized as generally three-stage growth structure based on growth bundles along the dichotomous growth axes that are assembled by multiple growth types (Figure 2). As an important aspect of coral growth, we consider a group of corallites that derives from the same corallite as a growth bundle, which contains all the above-described growth types, and the growth direction of the bundle depends on the growth axis direction of its branch.

Light plays a vital role during the growth of the corals. Different environmental conditions affected calice and inter-septal space structures within the same colony and they can be classified into low light and lighted mineralization areas, and low light and lighted growth areas based on modeling. The measurements in the calice and inter-septal space reconstruction (including diameter; volume; surface area; surface-volume ratio data; projected distances of the X, Y, and Z axes; and projected areas of the XY, XZ, and YZ planes) show apparent differences between light areas and low-light areas (Figure 3). The data show that polyps in light areas grow better than those in dark areas, reflected by larger average volume and surface area of calices and inter-septal spaces. The direction of coral growth axis also goes toward the light area, whereas the growth of the dark area slows gradually and eventually stops. Because all these calices and inter-septal spaces are in the same branchlet, which means that their nutrient availability and water-current direction are basically the same, this analysis demonstrates the importance of lights to coral growth. However, this does not mean that all polyps grow straight toward the light; instead, all polyps in a colony grow along the growth axis of their branch. Once the growth deviates from the growth axis, the polyp stops growing, immediately secrets its new calice. *P. damicornis* also has a macroscopic integral growth axis that contains branches. Polyps in a new branch grow along the new axis. In this growth pattern, the active area is exposed to light increases, which significantly enhances the light energy utilization of the coral and plays a vital role in the competition of lights against other marine organisms of the same ecological niche. This phenomenon reveals the relationship between the coral formation process and the adaptive evolution of corals in enhancing photosynthesis.

During the process of coral growth, new buddings grow chamber by chamber. When a polyp secrets a new calice, the polyp enters a newly created chamber. A macroscopic result of the formation of new chambers is a growth ring (Figure S4). Because adjacent calices share skeletons, adjacent polyps in the same growth ring have to maintain a synchronized growth rate. In this study, we visualize the growth ring of *Pocillopora*. Addressing the growth of other reef-building corals is of great interest, if we are to understand their growth patterns at monthly, seasonal, and yearly time scales in detail.

Calice-Reconstruction as a Method for Studying the Reef-Building Corals

Because the corallite structures and calice and inter-septal space network of *Pocillopora* are neat, we used *Pocillopora* as a model species to describe the method. The polyps in a *Pocillopora* colony build new calices from its budding point, which are significantly shown as inverted cone-shaped structures in the reconstruction. The process of polyp growth can be traced by studying the internal structure of the calices and inter-septal spaces; therefore, we can obtain the budding, growth, and distribution information of the polyps in a colony by reconstructions. Our study first records the growth patterns of *P. damicornis* based on the internal calice and inter-septal space network, which is poorly known from previous studies (Escalona et al., 1999; Bosch et al., 2010; Vizel et al., 2011). During the budding process of typical hydrozoans such as hydras and jellyfish (Schlesinger et al., 2010; Bosch, 2012), the new bud grows gradually upward, separated from the parents once it has a complete structure. In studies of the polyp network in these organisms, new buds are almost impossible to be traced after they are separated, making the growth and budding network of hydrozoans difficult to be studied. However, our study of *P. damicornis* by HRCT points out a potential solution to investigate the growth process of hydrozoans and their budding patterns.

Branches of *P. damicornis* are always dichotomous during the growth of the colony. There are no other exceptions observed in this study. The calice and inter-septal space of *P. damicornis* record the growth process of extending polyps; therefore, we can reconstruct the gradual growth of a colony. This investigation on the detailed growth process of *P. damicornis* by HRCT demonstrates the value of such method for understanding the coral body plan and the growth pattern of reef-building coral species.

Conclusions

Our work presents an application of cutting-edge technology in investigating reef-building coral structures and reconstructing the internal calice and inter-septal space network, based on a large corallum of *P. damicornis*. We studied the growth patterns of *P. damicornis* through the budding, growth, and distribution information obtained from the reconstruction of coral calice and inter-septal space network. It reveals that each calice of *P. damicornis* is a basic polyp growth unit, and growth bundles are arranged along the growth axis in a dichotomous branching pattern. The growth pattern of *P. damicornis* lays the

foundation for further explorations on the monthly, seasonal, and yearly growth of reef-building corals. Furthermore, we reconstruct the entire calice and inter-septal space network in *P. damicornis* by HRCT, which sheds light on studying the process of coral formation and budding patterns of living polyps. Our results also suggest that HRCT can be used to characterize the development and process of coral growth. To sum up, the three-dimensional morphological reconstruction on the calice and inter-septal space structures in *P. damicornis* reveal a method for studying the biological characteristics and growth patterns of reef-building coral species.

Ethics

All coral sample collecting and processing were performed according to the local laws governing the welfare of invertebrate animals and were approved by the Southeast University (SEU) ethical committee.

Limitations of the Study

It should be noted that the growth patterns listed in this study are based on the *P. damicornis* colony, so they may not be suitable for all coral species in *Pocillopora*. The method for studying the growth and budding patterns of coral species listed in this study can be used for many major reef-building coral genera like *Pocillopora*, *Acropora*, *Montipora*, and *Seriatopora*. However, there still could be some special coral species that cannot be studied through this method.

Resource Availability

Lead Contact

Further information and requests for resources and reagents should be directed to and will be fulfilled by the Lead Contact, Zuhong Lu (zhlu@seu.edu.cn).

Materials Availability

The HRCT data in this study have been deposited to the IVPP Digital data repository ADMorph [Archives of Digital Morphology, https://doi.org/10.12112/F.15].

Data and Code Availability

The CT data that support the findings of this study, as well as the 3D surface files, are available in the IVPP Digital data repository ADMorph (Archives of Digital Morphology, https://doi.org/10.12112/F.15).

The code used in ISODATA test can be found in Supplemental Information.

METHODS

All methods can be found in the accompanying Transparent Methods supplemental file.

SUPPLEMENTAL INFORMATION

Supplemental Information can be found online at https://doi.org/10.1016/j.isci.2020.101069.

ACKNOWLEDGMENTS

We thank Prof. M. Zhu from Institute of Vertebrate Paleontology and Paleoanthropology, CAS for technical and scientific guidance; Prof. M.-Y. Zhu from Nanjing Institute of Geology and Paleontology, CAS for scientific guidance; Y. Loya from the Israel Academy of Sciences for scientific guidance; and S. Yang from University of Rochester for paper editing. This work was supported by the State Key Laboratory Foundation of China (5507059002). J.L. is supported by the Strategic Priority Research Program of Chinese Academy of Sciences, Grant No. XDB26000000.

AUTHOR CONTRIBUTIONS

C.H., Z.L., Y.L., and J.L. conceived the project. Y.L., J.L., C.H., and Z.L. wrote the paper. Y.L. performed the micro-CT experiments and segmentation. Y.L., K.B., and C.H. performed the biological analyses. Y.L., T.H., J.L., and C.H. drew the figures. All authors discussed, wrote, and commented on the data.

DECLARATION OF INTERESTS

The authors declare no competing interests.

Received: July 18, 2019
Revised: October 9, 2019
Accepted: April 13, 2020
Published: June 26, 2020

REFERENCES

Adjeroud, M., Kayal, M., Iborra-Cantonnet, C., Vercelloni, J., Bosserelle, P., Liao, V., Chancerelle, Y., Claudet, J., and Penin, L. (2018). Recovery of coral assemblages despite acute and recurrent disturbances on a South Central Pacific reef. Sci. Rep. *8*, 9860.

Bellwood, D., Hughes, T., Folke, C., and Nyström, M. (2004). Confronting the coral reef crisis. Nature *429*, 827–833.

Ben-Haim, Y., Zicherman-Keren, M., and Rosenberg, E. (2003). Temperature-regulated bleaching and lysis of the coral *Pocillopora damicornis* by the novel pathogen *Vibrio coralliilyticus*. Appl. Environ. Microbiol. *69*, 4236–4242.

Beuck, L., Vertino, A., Stepina, E., Karolczak, M., and Pfannkuche, O. (2007). Skeletal response of *Lophelia pertusa* (Scleractinia) to bioeroding sponge infestation visualised with micro-computed tomography. Facies *53*, 157–176.

Bonesso, J.L., Leggat, W., and Ainsworth, T.D. (2017). Exposure to elevated sea-surface temperatures below the bleaching threshold impairs coral recovery and regeneration following injury. PeerJ *5*, e3719.

Bosch, T.C., Anton-Erxleben, F., Hemmrich, G., and Khalturin, K. (2010). The hydra polyp: nothing but an active stem cell community. Dev. Growth Differ. *52*, 15–25.

Bosch, T.C. (2012). What hydra has to say about the role and origin of symbiotic interactions. Biol. Bull. *223*, 78–84.

Bramanti, L., and Edmunds, P.J. (2016). Density-associated recruitment mediates coral population dynamics on a coral reef. Coral Reefs *35*, 543–553.

Brener-Raffalli, K., Clerissi, C., Vidal-Dupiol, J., Adjeroud, M., Bonhomme, F., Pratlong, M., Aurelle, D., Mitta, G., and Toulza, E. (2018). Thermal regime and host clade, rather than geography, drive *Symbiodinium* and bacterial assemblages in the scleractinian coral *Pocillopora damicornis* sensu lato. Microbiome *6*, 39.

Carpenter, K.E., Abrar, M., Aeby, G., Aronson, R.B., Banks, S., Bruckner, A., Chiriboga, A., Cortés, J., Delbeek, J.C., Devantier, L., et al. (2008). One-third of reef-building corals face elevated extinction risk from climate change and local impacts. Science *321*, 560–563.

Chindapol, N., Kaandorp, J.A., Cronemberger, C., Mass, T., and Genin, A. (2013). Modelling growth and form of the scleractinian coral *Pocillopora verrucosa* and the influence of hydrodynamics. PLoS Comput. Biol. *9*, e1002849.

Combosch, D.J., and Vollmer, S.V. (2013). Mixed asexual and sexual reproduction in the Indo-Pacific reef coral *Pocillopora damicornis*. Ecol. Evol. *3*, 3379–3387.

Combosch, D.J., and Vollmer, S.V. (2015). Trans-Pacific RAD-Seq population genomics confirms introgressive hybridization in Eastern Pacific *Pocillopora* corals. Mol. Phylogenet. Evol. *88*, 154–162.

Costanza, R., de Groot, R., Sutton, P., van der Ploeg, S., Anderson, S.J., Kubiszewski, I., Farber, S., and Turner, R.K. (2014). Changes in the global value of ecosystem services. Glob. Environ. Chang. *26*, 152–158.

Crowder, C.M., Liang, W.L., Weis, V.M., and Fan, T.Y. (2014). Elevated temperature alters the lunar timing of planulation in the brooding coral *Pocillopora damicornis*. PLoS One *9*, e107906.

Crowder, C.M., Meyer, E., Fan, T.Y., and Weis, V.M. (2017). Impacts of temperature and lunar day on gene expression profiles during a monthly reproductive cycle in the brooding coral *Pocillopora damicornis*. Mol. Ecol. *26*, 3913–3925.

Cunning, R., and Baker, A.C. (2012). Excess algal symbionts increase the susceptibility of reef corals to bleaching. Nat. Clim. Chang. *3*, 259.

Cunning, R., Bay, R.A., Gillette, P., Baker, A.C., and Traylor-Knowles, N. (2018). Comparative analysis of the *Pocillopora damicornis* genome highlights role of immune system in coral evolution. Sci. Rep. *8*, 16134.

De'ath, G., Fabricius, K.E., Sweatman, H., and Puotinen, M. (2012). The 27-year decline of coral cover on the Great Barrier Reef and its causes. Proc. Natl. Acad. Sci. U S A *109*, 17995–17999.

Ellison, A.M., Bank, M.S., Clinton, B.D., Colburn, E.A., Elliott, K., Ford, C.R., Foster, D.R., Kloeppel, B.D., Knoepp, J.D., Lovett, G.M., et al. (2005). Loss of foundation species: consequences for the structure and dynamics of forested ecosystems. Front. Ecol. Environ. *3*, 479–486.

Escalona, M., Lorenzo, J.C., González, B., Daquinta, M., González, J.L., Desjardins, Y., and Borroto, C.G. (1999). Pineapple (*Ananas comosus* L. Merr) micropropagation in temporary immersion systems. Plant Cell Rep. *18*, 743–748.

Fabricius, K.E., Okaji, K., and De'ath, G. (2010). Three lines of evidence to link outbreaks of the crown-of-thorns seastar *Acanthaster planci* to the release of larval food limitation. Coral Reefs *29*, 593–605.

Graham, N.A. (2014). Habitat complexity: coral structural loss leads to fisheries declines. Curr. Biol. *24*, R359–R361.

Helman, Y., Natale, F., Sherrell, R.M., Lavigne, M., Starovoytov, V., Gorbunov, M.Y., and Falkowski, P.G. (2008). Extracellular matrix production and calcium carbonate precipitation by coral cells in vitro. Proc. Natl. Acad. Sci. U S A *105*, 54–58.

Janiszewska, K., Stolarski, J., Benzerara, K., Meibom, A., Mazur, M., Kitahara, M.V., and Cairns, S.D. (2011). A unique skeletal microstructure of the deep-sea micrabaciid scleractinian corals. J. Morphol. *2*, 191–203.

Janiszewska, K., Jaroszewicz, J., and Stolarski, J. (2013). Skeletal ontogeny in basal scleractinian micrabaciid corals. J. Morphol. *3*, 243–257.

Johnston, E.C., Forsman, Z.H., Flot, J.F., Schmidt-Roach, S., Pinzón, J.H., Knapp, I.S.S., and Toonen, R.J. (2017). A genomic glance through the fog of plasticity and diversification in *Pocillopora*. Sci. Rep. *7*, 5991.

Jokiel, P.L., and Coles, S.L. (1977). Effects of temperature on the mortality and growth of Hawaiian reef corals. Mar. Biol. *43*, 201–208.

Kayal, M., Vercelloni, J., Wand, M.P., and Adjeroud, M. (2015). Searching for the best bet in life-strategy: a quantitative approach to individual performance and population dynamics in reef-building corals. Ecol. Complex. *23*, 73–84.

Kleypas, J.A., Buddemeier, R.W., Archer, D., Gattuso, J.P., Langdon, C., and Opdyke, B.N. (1999). Geochemical consequences of increased atmospheric carbon dioxide on coral reefs. Science *284*, 118–120.

Knackstedt, M.A., Arns, C.H., Senden, T.J., and Gross, K. (2006). Structure and properties of clinical coralline implants measured via 3D imaging and analysis. Biomaterials *27*, 2776–2786.

Knowlton, N., Brainard, R.E., Fisher, R., Moews, M., and Caley, M.J. (2010). Coral reef biodiversity. In Life in the World's Oceans: Diversity Distribution and Abundance, A.D. McIntyre, ed. (Wiley-Blackwell), pp. 65–74.

Kopp, C. (2015). Subcellular investigation of photosynthesis-driven carbon assimilation in the symbiotic reef coral *Pocillopora damicornis*. MBio *10*, 6.

Kruszynski, K., Liere, R.V., and Kaandorp, J.A. (2006). An Interactive Visualization System for Quantifying Coral Structures (The Eurographics Association).

Kruszynski, K., Kaandorp, J.A., and Liere, R.V. (2007). A computational method for quantifying morphological variation in scleractinian corals. Coral Reefs *26*, 831–840.

Kvitt, H., Kramarsky-Winter, E., Maor-Landaw, K., Zandbank, K., Kushmaro, A., Rosenfeld, H., Fine, M., and Tchernov, D. (2015). Breakdown of coral colonial form under reduced pH conditions is initiated in polyps and mediated through apoptosis. Proc. Natl. Acad. Sci. U S A *112*, 2082–2086.

Lecointe, A., Cohen, S., Gèze, M., Djediat, C., Meibom, A., and Domart-Coulon, I. (2013). Scleractinian coral cell proliferation is reduced in primary culture of suspended multicellular aggregates compared to polyps. Cytotechnology *65*, 705–724.

Mass, T., Drake, J.L., Haramaty, L., Rosenthal, Y., Schofield, O.M., Sherrell, R.M., and Falkowski, P.G. (2012). Aragonite precipitation by proto-polyps in coral cell cultures. PLoS One *7*, e35049.

Mass, T., Putnam, H.M., Drake, J.L., Zelzion, E., Gates, R.D., Bhattacharya, D., and Falkowski, P.G. (2016). Temporal and spatial expression patterns of biomineralization proteins during early development in the stony coral *Pocillopora damicornis*. Proc. Biol. Sci. *27*, 283.

Maynard, J., van Hooidonk, R., Eakin, C.M., Puotinen, M., Garren, M., Williams, G., Heron, S.F., Lamb, J., Weil, E., Willis, B., et al. (2015). Projections of climate conditions that increase coral disease susceptibility and pathogen abundance and virulence. Nat. Clim. Chang. *5*, 688.

Miller, K.J., and Ayre, D.J. (2004). The role of sexual and asexual reproduction in structuring high latitude populations of the reef coral *Pocillopora damicornis*. Heredity (Edinb.) *92*, 557–568.

Mollica, N.R. (2018). Ocean acidification affects coral growth by reducing skeletal density. Proc. Natl. Acad. Sci. U S A *115*, 1754–1759.

Mu, J., Zhao, X., Li, J., Yang, E.C., and Zhao, X.J. (2017). Coral-like CeO_2/NiO nanocomposites with efficient enzyme-mimetic activity for biosensing application. Mater. Sci. Eng. C. Mater. Biol. Appl. *74*, 434–442.

Natt, M., Lönnstedt, O.M., and McCormick, M.I. (2017). Coral reef fish predator maintains olfactory acuity in degraded coral habitats. PLoS One *12*, e0179300.

Nishikawa, T., Okamura, T., Masuno, K., Tominaga, K., Wato, M., Kokubu, M., Imai, K., Takeda, S., Hidaka, M., and Tanaka, A. (2009). Physical characteristics and interior structure of coral skeleton as a bone scaffold material. J. Oral. Tissue Eng. *7*, 121–127.

Paz-García, D.A., Hellberg, M.E., García-de-León, F.J., and Balart, E.F. (2015). Switch between morphospecies of *Pocillopora* corals. Am. Nat. *186*, 434–440.

Rivest, E.B., and Hofmann, G.E. (2014). Responses of the metabolism of the larvae of *Pocillopora damicornis* to ocean acidification and warming. PLoS One *9*, e96172.

Robinson, J.P., Williams, I.D., Edwards, A.M., McPherson, J., Yeager, L., Vigliola, L., Brainard, R.E., and Baum, J.K. (2017). Fishing degrades size structure of coral reef fish communities. Glob. Chang. Biol. *23*, 1009–1022.

Rodríguez-Villalobos, J.C., Work, T.M., and Calderon-Aguilera, L.E. (2016). Wound repair in *Pocillopora*. J. Invertebr. Pathol. *139*, 1–5.

Schlesinger, A., Kramarsky-Winter, E., Rosenfeld, H., Armoza-Zvoloni, R., and Loya, Y. (2010). Sexual plasticity and self-fertilization in the sea anemone *Aiptasia diaphana*. PLoS One *5*, e11874.

Schmidt-Roach, S., Miller, K.J., and Lundgren, P. (2014). With eyes wide open: a revision of species within and closely related to the *Pocillopora damicornis* species complex (Scleractinia; Pocilloporidae) using morphology. Zool. J. Linn. Soc. https://doi.org/10.1111/zoj.12092.

Schmidt-Roach, S., Miller, K.J., Woolsey, E., Gerlach, G., and Baird, A.H. (2012). Broadcast spawning by *Pocillopora* species on the great barrier reef. PLoS One *7*, e50847.

Schmidt-Roach, S., Lundgren, P., Miller, K.J., Gerlach, G., Noreen, A.M.E., and Andreakis, N. (2013). Assessing hidden species diversity in the coral *Pocillopora damicornis* from Eastern Australia. Coral Reefs *32*, 161–172.

Shapiro, O.H., Kramarsky-Winter, E., Gavish, A.R., Stocker, R., and Vardi, A. (2016). A coral-on-a-chip microfluidic platform enabling live-imaging microscopy of reef-building corals. Nat. Commun. *7*, 10860.

Souter, P., Henriksson, O., Olsson, N., and Grahn, M. (2009). Patterns of genetic structuring in the coral *Pocillopora damicornis* on reefs in East Africa. BMC Ecol. *9*, 19.

Stoddart, J.A. (1984). Genetical structure within populations of the coral *Pocillopora damicornis*. Mar. Biol. *81*, 19–30.

Szabó, M., Wangpraseurt, D., Tamburic, B., Larkum, A.W., Schreiber, U., Suggett, D.J., Kühl, M., and Ralph, P.J. (2014). Effective light absorption and absolute electron transport rates in the coral *Pocillopora damicornis*. Plant Physiol. Biochem. *83*, 159–167.

Tambutté, E., Venn, A.A., Holcomb, M., Segonds, N., Techer, N., Zoccola, D., Allemand, D., and Tambutté, S. (2015). Morphological plasticity of the coral skeleton under CO2-driven seawater acidification. Nat. Commun. *6*, 7368.

Thomas, L., Kennington, W.J., Evans, R.D., Kendrick, G.A., and Stat, M. (2017). Restricted gene flow and local adaptation highlight the vulnerability of high-latitude reefs to rapid environmental change. Glob. Chang. Biol. *23*, 2197–2205.

Torda, G., Schmidt-Roach, S., Peplow, L.M., Lundgren, P., and van Oppen, M.J. (2013). A rapid genetic assay for the identification of the most common *Pocillopora damicornis* genetic lineages on the Great Barrier Reef. PLoS One *8*, e58447.

Traylor-Knowles, N. (2016). Distinctive wound-healing characteristics in the corals *Pocillopora damicornis* and *Acropora hyacinthus* found in two different temperature regimes. Mar. Biol. *163*, 231.

Veron, J.E.N., and Pichon, M. (1976). Scleractinia of Eastern Australia Part 1, Families Thamnasteriidae, Astrocoeniidae, Pocilloporidae, *1* (Australian Institute of Marine Science Monongraph), pp. 1–86.

Veron, J.E.N., and Staffordsmith, M. (2000). Corals of the World (Australian Institute of Marine Science).

Vizel, M., Loya, Y., Downs, C., and Kramarsky-Winter, E. (2011). A novel method for coral explant culture and micropropagation. Mar. Biotechnol. *13*, 423–432.

Weis, V., Davy, S., Hoegh-Guldberg, O., Rodriguez-Lanetty, M., and Pringle, J. (2008). Cell biology in model systems as the key to understanding corals. Trends Ecol. Evol. *23*, 369–376.

Wells, J.W. (1969). The Formation of Dissepiments in Zoanthrarian Corals (Australian National University Press), pp. 17–26.

Welsh, R.M., Rosales, S.M., Zaneveld, J.R., Payet, J.P., McMinds, R., Hubbs, S.L., and Thurber, R.L.V. (2017). Alien vs. predator: bacterial challenge alters coral microbiomes unless controlled by *Halobacteriovorax* predators. PeerJ *5*, e3315.

Wilkinson, S.P., Fisher, P.L., van, Oppen, M.J., and Davy, S.K. (2015). Intra-genomic variation in symbiotic dinoflagellates: recent divergence or recombination between lineages? BMC. Evol. Biol. *15*, 46.

Yu, X., Huang, B., Zhou, Z., Tang, J., and Yu, Y. (2017). Involvement of caspase3 in the acute stress response to high temperature and elevated ammonium in stony coral *Pocillopora damicornis*. Gene *637*, 108–114.

Yuan, C., Zhou, Z., Zhang, Y., Chen, G., Yu, X., Ni, X., Tang, J., and Huang, B. (2017). Effects of elevated ammonium on the transcriptome of the stony coral P*ocillopora damicornis*. Mar. Pollut. Bull. ***114***, 46–52.

Zhang, Y., Zhou, Z., Wang, L., and Huang, B. (2018). Transcriptome, expression, and activity analyses reveal a vital heat shock protein 70 in the stress response of stony coral *Pocillopora damicornis*. Cell Stress Chaperones *23*, 711–721.

Zhou, J., Fan, T.Y., Beardall, J., and Gao, K. (2016). Incident ultraviolet irradiances influence physiology, development and settlement of larva in the coral *Pocillopora damicornis*. Photochem. Photobiol. *92*, 293–300.

Zhou, Z., Yu, X., Tang, J., Zhu, Y., Chen, G., Guo, L., and Huang, B. (2017). Dual recognition activity of a rhamnose-binding lectin to pathogenic bacteria and zooxanthellae in stony coral *Pocillopora damicornis*. Dev. Comp. Immunol. *70*, 88–93.

Zhou, Z., Yu, X., Tang, J., Wu, Y., Wang, L., and Huang, B. (2018). Systemic response of the stony coral *Pocillopora damicornis* against acute cadmium stress. Aquat. Toxicol. *194*, 132–139.

iScience, Volume *23*

Supplemental Information

The 3D Reconstruction of *Pocillopora* Colony Sheds Light on the Growth Pattern of This Reef-Building Coral

Yixin Li, Tingyu Han, Kun Bi, Kun Liang, Junyuan Chen, Jing Lu, Chunpeng He, and Zuhong Lu

1. Transparent Methods

Specimen Collection

P. damicornis in this study was collected from the South China Sea in 2018 (Figure S1). The coral sample was kept whole and housed in our laboratory coral tank, where all conditions simulated its habitat in the South China Sea. This *P. damicornis* is lavender-red in colour. Its main branches are about 3.0 cm thick, spreading irregularly upward. In the wild, the polyps emerge from the calices on the coral surface and sway with the current. When external stimulation occurs, such as physical impact or removal from seawater, the polyps immediately shrink into their calices, eventually returning to their original state after a period.

Coral Culture System

P. damicornis is cultured in a standard RedSea® tank (redsea575, Red Sea Aquatics Ltd). The temperature is kept at 25° C and the salinity (Red Sea Aquatics Ltd) is 1.025. The culture system is maintained by a Protein Skimmer (regal250s, Reef Octopus), a water chiller (tk1000, TECO Ltd), three coral lamps (AI®, Red Sea Aquatics Ltd), two wave devices (VorTech^{TM} MP40, EcoTech Marine Ltd), and calcium reactor (Calreact 200, Reef Octopus) etc.

X-ray Microtomography

We analysed three specimens (specimens 2 and 3 were separated from specimen 1) from the South China Sea. All CT scanning was performed using a v|tome|x M (General Electric, Milwaukee, WI) at Yinghua NDT, Shanghai, China.

Specimen 1 was scanned with a beam energy of 210 kV and a flux of 205 μA at a detector resolution of 87 μm per pixel, using a 360° rotation with a step size of 0.18°. A total of 2,000 transmission images were reconstructed in a 2,000 × 2,000 matrix of 2,000 slices in a two-dimensional reconstruction software developed by GE. Specimen 2 was scanned with a beam energy of 220 kV and a flux of 120 μA at a detector resolution of 18 μm per pixel, using a 360° rotation with a step size of 0.164°. A total of 2,200 transmission images were reconstructed in a 2,000 × 2,000 matrix of 2,000 slices in a two-dimensional reconstruction software developed by GE. Specimen 3 was scanned with a beam energy of 180 kV and a flux of 130 μA at a detector resolution of 16 μm per pixel, using a 360° rotation with a step size of 0.24°.

A total of 1,500 transmission images were reconstructed in a 2,000 × 2,000 matrix of 2,000 slices in a two-dimensional reconstruction software developed by GE. Image sections and 3D rendered images was performed using VG StudioMax Version 3.2 (Volume Graphics).

High-resolution computed tomography used in reef-building coral research

Our work presents a novel use of high-resolution computed tomography (HRCT) for studying reef-building coral structures. HRCT can nondestructively capture the appearance and internal structure of corals (Figure 1, Figure S5). Compared with traditional biological techniques, such as bailout, SEM, and grinding sections, HRCT has multiple advantages in this study.

First, this method does not require complicated and potentially destructive preparations such as pickling or fixing and can even be used directly on living corals. HRCT reveals the delicate internal skeletal structures in *P. damicornis* that are easily destroyed during electron microscope observation and grinding.

Second, traditional biological techniques are unable to determine the size of the polyp calice. Corrosion of the coral skeleton caused by pickling before grinding will distort measurement results, while the fixing process before electron microscopy also causes deformation of the coral skeleton. Polyps obtained by bailout will shrink upon the loss of the support of the skeleton and therefore do not display the true scale of the calice. However, we can effortlessly measure the internal coral skeleton width with microtomography, naturally obtaining the diameter of the polyp oral surface and the true size of the calice.

At the same time, high-resolution images can be obtained by microtomography, with resolutions up to 10 μm for samples of 10 cm^3 and resolutions of approximately 80 μm for large colonies of 3,600 cm^3, these resolutions are unmatched by other methods. Finally, because microtomography can capture all coral structural information in detail at once, we can observe any position and section in a colony as needed, saving coral resources and eliminating the burden of multiple measurements while deriving a complete analysis of a sample. Our results therefore suggest that large-scale microtomography technology can be used to characterize the development and progress of coral structural growth, filling in the gaps in current coral studies and making significant contributions to ecological biology research of marine organisms and habitats.

Scanning Electron Microscopy (SEM)

Polyp sample collection was run as previously described (Shapiro et al., 2016). A small branch tip (5-10 mm) is removed from the mother colony using a clean stainless-steel bone cutter. The branch tip is placed in an open glass Petri dish filled with filtered artificial seawater just covering the coral fragment. A gradual increasing salinity concentration results in a polyp bail-out response, which make polyps released from the coral skeleton due to water evaporation. One 5-10 mm *P. damicornis* branch can yield 30–40 polyps within 48 hours. The bail-out polyps were fixed with 2.5% glutaric dialdehyde in 0.035M PBSNa, and general SEM experimental steps were run as previously described (Chindapol et al., 2013).

Iterative Self-organizing Data Analysis (ISODATA)

ISODATA, which has been widely used as a clustering algorithm (Mingchao et al., 2017), is used to divide the calices and inter-septal spaces into different polyp growth patterns in this work. As an unsupervised classification algorithm, ISODATA has the advantage of permitting an unknown number of clusters (Boudraa et al., 1992; Velasco et al., 2007) to be specified rather than requiring that value to be known *a priori* in the k-means algorithm method (Ahmad et al., 2013). The ISODATA algorithm uses the following process: (1) set initial parameters. (2) Calculate the distance index function of each cluster. (3) Merge or split the clusters according to the given requirements. (4) Repeat iteratively, calculating new indexes and determining whether the results meet the clustering requirements (Code can be seen in the Supplemental Information). In this study, the input dataset is set as thirteen data layers for each coral chamber, including the diameter, volume, surface area, surface

area/volume, the spatial coordinates of the X, Y, and Z axes, the projected distance along the X, Y and Z axes, and projected areas on the XY, XZ and YZ planes. Then two sample t-tests are used for the characteristics of different patterns, including the diameter, volume, surface area, surface area/volume, projected distance along X, Y and Z axes and projected areas on the XY, XZ and YZ planes.

2. Supplemental Figures

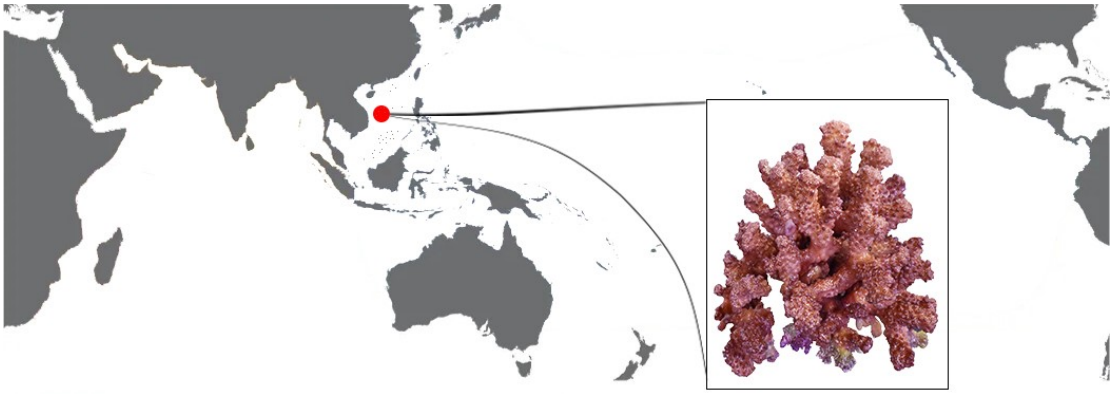

Figure S1 Sample location of the *Pocillopora* colony used in this study. Related to Figure 1 *P. damicornis* in this study was collected from the Xisha Islands (latitude 15°40'–17°10' north, longitude 111°—113° east), shown as a red dot at the centre of the map.

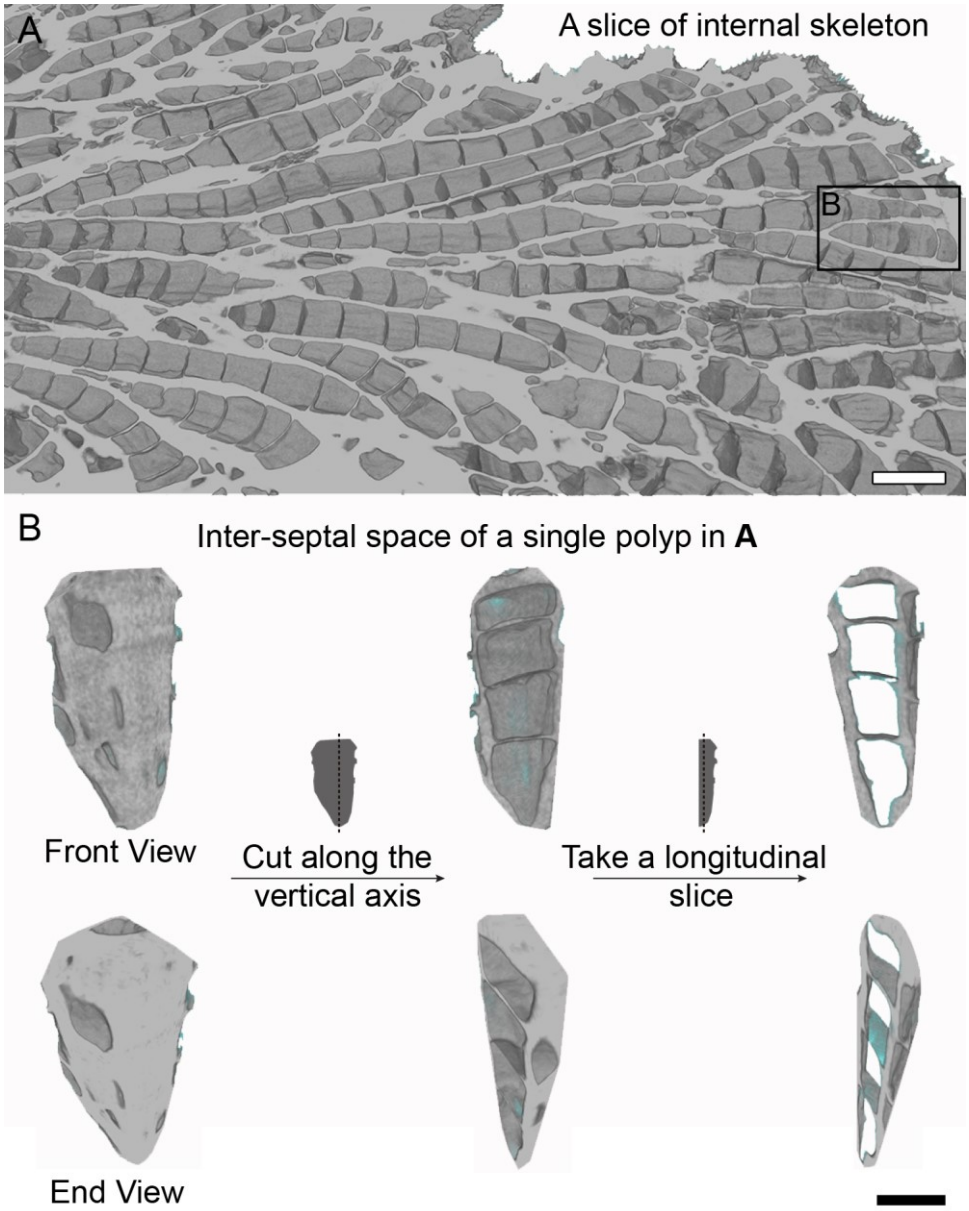

Figure S2 Schematic diagram of *P. damicornis* skeleton reconstruction. Related to Figure 1 (A) Sectional view of coral branch reconstruction. The bamboo-like calice and inter-septal space structures on the same branch is arranged in a generally alternate pattern. (B) We selected the calice and inter-septal space structures of a single polyp in **A**. To show its internal structure, we cut it along the vertical axis to expose the inter-septal spaces inside. For a more detailed observation, we took a longitudinal slice and find that there are some transparent sites along the extremely thin dissepiments, so that the various calices mineralized by one independent polyp are connected. Scale bars: (A) 1 mm; (B) 0.5 mm.

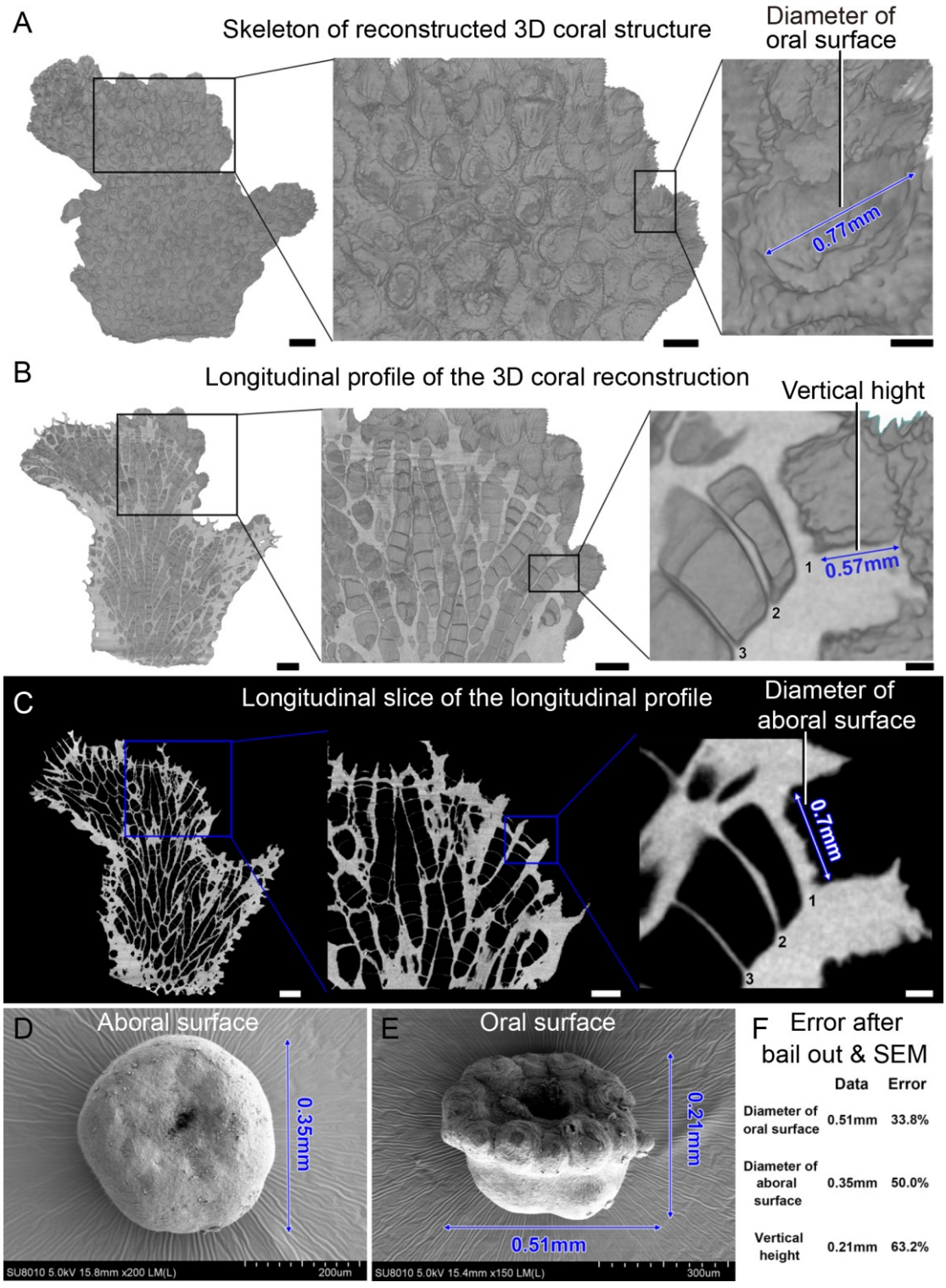

Figure S3 Related to Figure 1 Measuring the scale of a *P. damicornis* polyp calices with micro-CT. (A-C) We can directly measure the natural size of a calice in the 3D reconstruction, 3D profile and 3D slice produced by X-ray microfocus computed tomography. **A** is a reconstructed 3D structure, **B** is a longitudinal profile of the 3D reconstruction. **C** is a longitudinal slice of the longitudinal profile. (D, E) Scanning electron microscope (SEM) image of a *P. damicornis* polyp obtained by polypbail out (see Reference 1 for methodology). Polyps obtained by bailout shrink because they lose skeletal support, while the fixing process before SEM causes polyp

deformation, which distorts the true scale of the polyp calice. **D** is the SEM image of a polyp's abactinal surface. **E** is the SEM image of a polyp's oral surface. (F) Measuring error after polyp bailout and SEM. **A**-**C** Data are represented as mean ±HRCT. **D**, **E** Data are represented as mean ±SEM. Scale bars: (A) 2 mm, (B) 1 mm, (C) 0.2 mm; (D) 200 μm; (E) 300 μm.

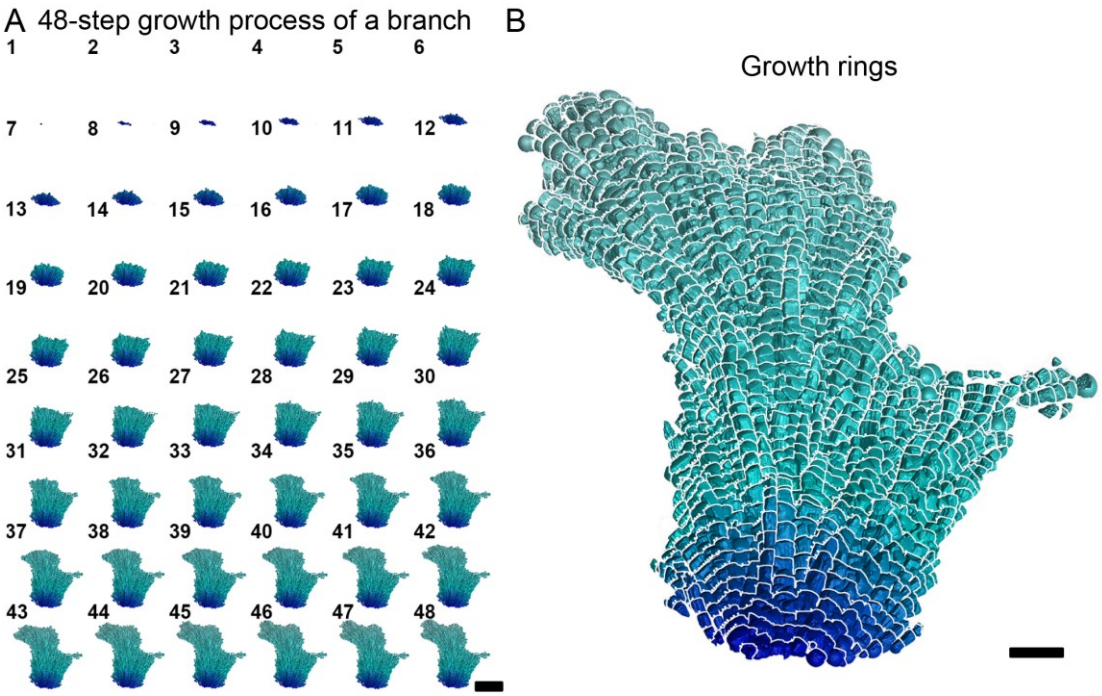

Figure S4 The 48-step growth process and growth rings of a branch of *P. damicornis*. Related to Figure 2 (A) By reconstructing all the pore canals in a single *P. damicornis* branch, and dividing the entire growth process into 48 strata according to the coral branch's horizontal synchronisation, we can present the growth process of *P. damicornis* directly. (B) By simulating the 48-step growth process of a *P. damicornis* branch, we can visualise its growth rings, showing how the *Pocillopora* grew and enabling research into the yearly, seasonal, and monthly growth of reef-building corals. Scale bars: (A) 1 mm; (B) 2 mm.

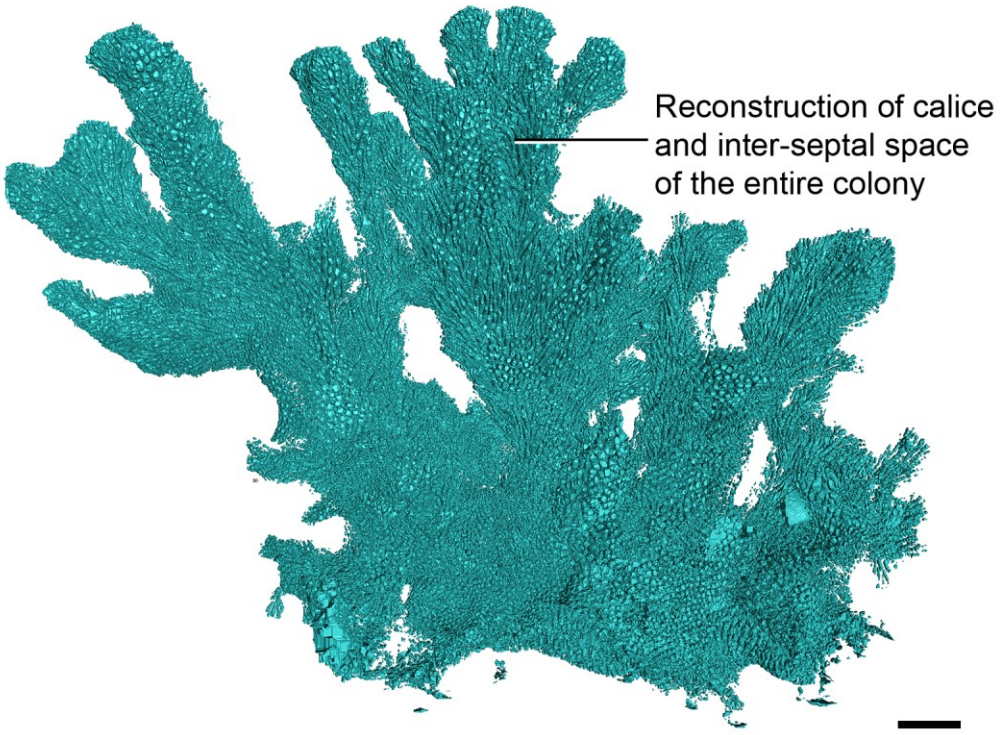

Figure S5 The reconstruction of calice and inter-septal space of the entire colony in Fig. 1A. Related to Figure 2 Scale bar: 1 cm.

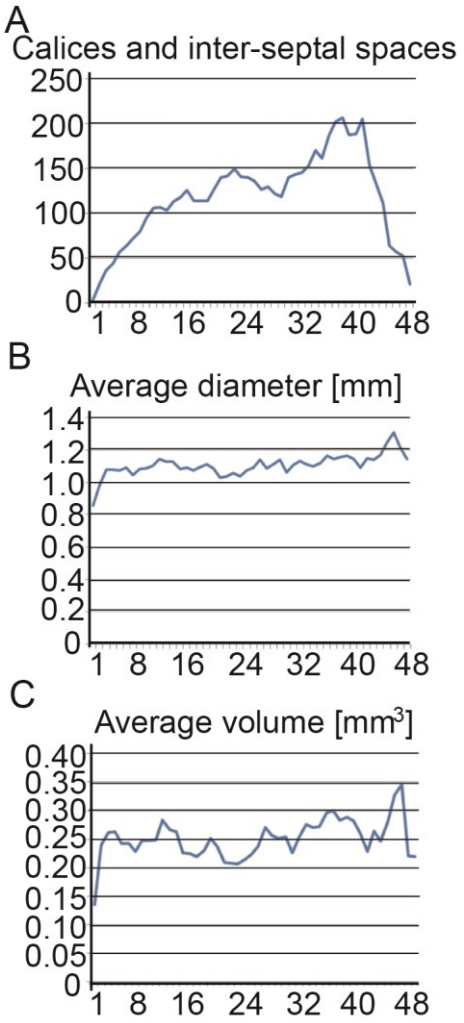

Figure S6 Line charts of calices, average diameter and average volume of calices in 48 layers. Related to Figure 3 (A) Calices and inter-septal space line chart. (B) Average diameter line chart. (C) Average volume line chart. Data are represented as mean ±HRCT.

3. Supplemental Table

Supplementary Table 1 Related to Figure 3 | Everage diameter and volume of calices between dissepiments in the 48-layer *P.damicornis* colony. Data are represented as mean ±HRCT.

Layer	Calices and inter-septal space	Average diameter [mm]	Average volume [mm³]
1	2	0.855	0.135
2	21	0.986	0.240
3	36	1.077	0.262
4	44	1.079	0.263
5	57	1.073	0.243
6	64	1.092	0.243
7	72	1.045	0.229

8	80	1.082	0.248
9	95	1.088	0.248
10	106	1.103	0.249
11	107	1.146	0.283
12	104	1.126	0.267
13	113	1.127	0.263
14	118	1.081	0.226
15	126	1.090	0.225
16	114	1.073	0.219
17	114	1.095	0.230
18	114	1.110	0.252
19	127	1.086	0.237
20	140	1.031	0.210
21	142	1.038	0.208
22	150	1.058	0.207
23	141	1.038	0.214
24	140	1.075	0.223
25	136	1.089	0.237
26	127	1.141	0.271
27	130	1.087	0.257
28	122	1.110	0.251
29	119	1.141	0.254
30	140	1.064	0.226
31	143	1.108	0.253
32	146	1.133	0.276
33	153	1.113	0.271
34	170	1.101	0.272
35	162	1.118	0.296
36	187	1.166	0.300
37	202	1.143	0.284
38	207	1.157	0.288
39	188	1.166	0.282
40	189	1.143	0.261
41	205	1.092	0.228
42	154	1.148	0.264
43	134	1.140	0.247
44	112	1.171	0.281
45	64	1.247	0.327
46	57	1.309	0.346
47	53	1.214	0.221
48	21	1.146	0.220

4. Supplemental Code

Data S1 Related to Figure 3 | The entire code of ISODATA analysis:

```
function [centroid, result] = ISODATA(data, iteration, desired_k, minimum_n,
maximum_variance, minimum_d,centroid)

% Pre-allocate result
distance_matrix = zeros(size(data,1), desired_k);
result = zeros(size(data,1),1);

for i = 1 : iteration
    previous_centroid = centroid;
    for j = 1 : size(distance_matrix,1)
        for k = 1 : size(distance_matrix,2)
            distance_matrix(j,k) = sqrt(sum((data(j,:)-centroid(k,:)) .^ 2));
        end
    end
    [~,result] = min(distance_matrix,[],2);

    % Whether the number of points in each class is smaller than minimum_n
    for j = 1 : size(centroid, 1)
        if(isempty(find(result == j,1)) || (size(find(result == j),1) < minimum_n))

            % One class with number of points in it less than minimum_n
            % should be deleted, along with records in the distance_matrix
            centroid(j,:) = [];
            distance_matrix(:,j) = [];

            % Re-assign each point to its closet neighbor class
            [~,result] = min(distance_matrix,[],2);
```

```
            % Recalculate centroids
            for k = 1:size(centroid,1)
                centroid(k,:) = mean(data(result(:,1) == k,:));
            end
        end
    end

    % Check if combining and splitting are needed
    % Case 1: too few classes
    if(size(centroid,1) <= (desired_k/2))
        % Split
        [centroid] = ISODATA_split(data, centroid, result, minimum_n,
maximum_variance);

    % Case 2: too many classes
    elseif(size(centroid,1) > (2*desired_k))
        % Combine
        [centroid] = ISODATA_combine(centroid, result, minimum_d);

    end

    if(previous_centroid == centroid)
        fprintf('Clustering over after %i iterations...\n', i);
        break;
    end
end
```

```
end


% Splitting

function [centroid] = ISODATA_split(data, centroid, current_result, minimum_n,
maximum_variance)


[centroid_x, centroid_y] = size(centroid);


variance_matrix = zeros(centroid_x, centroid_y); % pre-allocate the variance matrix


for i = 1 : centroid_x

    for j = 1 : centroid_y

        variance_matrix(i,j) = var(data(current_result == i,j));

    end

end


class_variance = max(variance_matrix,[],2); % find the greatest one-dimension
variance per class


for i = 1 : centroid_x

    if((class_variance(i,1) > maximum_variance) && size(find(current_result ==
i),1) > (2*minimum_n))


        % The current class should be splitted into two different classes

        centroid(i,:) = centroid(i,:) + sqrt(maximum_variance);

        centroid(end+1,:) = centroid(i,:) - sqrt(maximum_variance); % add one new
class to centroid set

    end
```

```
end
end

% Combining
function [centroid] = ISODATA_combine(centroid, current_result, minimum_d)
centroid_x = size(centroid,1);
class_distance_matrix = zeros(centroid_x, centroid_x);

% Calculate distances between two different classes
for i = 1 : x
    for j = 1 : x
        if(i ~= j)
            class_distance_matrix(i,j) = sqrt(sum((centroid(i,:)-centroid(j,:)) .^ 2));
        end
    end
end

% Combining two classes
for i = 1 : x
    for j = 1 : x
        if((i ~= j) && (class_distance_matrix(i,j) <    minimum_d))
            n1 = size(find(current_result == i),1);
            n2 = size(find(current_result == j),1);
            centroid(i,:) = (1/(n1+n2)) * (n1 * centroid(i,:) + n2 * centroid(j,:));
            centroid(j,:) = [];
            break; % the number of combining operation is limited to 1 within
each iteration
```

```
            end
        end
    end


End
```

6. Supplemental References

Shapiro, O. H., Kramarsky-Winter, E., Gavish, A. R., Stocker, R., Vardi, A. (2016). A coral-on-a-chip microfluidic platform enabling live-imaging microscopy of reef-building corals. *Nat. Commun*. **7**, 10860.

Chindapol, N., Kaandorp, J. A., Cronemberger, C., Mass, T., Genin, A. (2013). Modelling growth and form of the scleractinian coral *Pocillopora verrucosa* and the influence of hydrodynamics. *PLoS Comput. Biol.* **9**, e1002849.

Mingchao, L., Shuai, H., Jonathan S. (2017). An enhanced ISODATA algorithm for recognizing multiple electric appliances from the aggregated power consumption dataset. *Energy Build.* **140**, 305–316.

Boudraa, A. E. O. *et al*. (1992). Automatic left ventricular cavity detection using fuzzy ISODATA and connected-components labeling algorithms. *Conf. Proc. IEEE Eng. Med. Biol. Soc.* **2**, 1895–1896.

Velasco, F. R. D. (2007). Thresholding using the ISODATA clustering algorithm. *IEEE Trans. Syst. Man Cybern.* **10**, 771–774.

Ahmad, A., Sufahani, S. F. (2013). Analysis of Landsat 5^{TM} data of Malaysian land covers using ISODATA clustering technique. *Applied Electromagnetics*.